

The Catalytic Pathways of Hydrohalogenation over Metal-Free Nitrogen-Doped Carbon Nanotubes

Kai Zhou,^[a] Bo Li,^[b] Qiang Zhang,^[a] Jia-Qi Huang,^[a] Gui-Li Tian,^[a] Jin-Chao Jia,^[a] Meng-Qiang Zhao,^[a] Guo-Hua Luo,^[a] Dang Sheng Su,^{*,[b, c]} and Fei Wei^{*,[a]}

Nitrogen-doped carbon nanotubes (N-CNTs) are found to be active as one novel heterogeneous catalyst for acetylene hydrochlorination reaction, possessing good activity ($\text{TOF} = 2.3 \times 10^{-3} \text{ s}^{-1}$) and high selectivity ($>98\%$). Compared to toxic and energy-consuming conventional catalysts, such as HgCl_2 , N-CNTs are more favorable in terms of sustainability, because of their thermo-stability, metal-free make up, and the wide availability of bulk CNT. Coupling X-ray photoelectron spectroscopy and density functional theory computations (DFT), the main active source and reaction pathway are shown. Good linearity between the quaternary nitrogen content and conversion is revealed. DFT study shows that the nitrogen doping enhanced the formation of the covalent bond between C_2H_2 and NCNT compared with the undoped CNT, and therefore promoted the addition reaction of the C_2H_2 and HCl into $\text{C}_2\text{H}_3\text{Cl}$.

A hydrohalogenation reaction involves the electrophilic addition of hydrohalic acids such as hydrogen chloride or hydrogen bromide to alkenes and alkynes to yield the corresponding halogenated compounds. Hydrohalogenation is a very important reaction for organic synthesis and the production of halogen-containing organic compounds. For example, heterogeneously catalyzed addition of HCl to acetylene/ethylene is a synthetic route for the production of monomer vinyl chloride (VCM), and the as-obtained VCM is polymerized into polyvinyl chloride (PVC). There are two employed industrially routes to produce VCM. One is pyrolysis of dichloroethane, which is synthesized by an addition reaction between ethylene and chlor-

ine, and the other is the calcium carbide method (hydrochlorination of acetylene) catalyzed by HgCl_2 . The use of mercury in VCM is not considered sustainable in Europe. However, Hg-based catalysts are widely employed in China. In 2013 global PVC production capacity was 50.9 Mta^{-1} , with PR China occupying a 41% share. As the world's largest producer, the 12.3 Mta^{-1} PVC is derived by the calcium carbide method catalyzed by HgCl_2 .^[1] Owing to the low heat transfer efficiency of fixed-bed reactors, they easily forms hot spots of over 200°C , and hence accelerate run-off of highly volatile mercury-involved catalysts. It is estimated that the production of 1.0 t of PVC consumes 1.02–1.41 kg HgCl_2 catalyst (HgCl_2 content: 10–12 wt%), while over 25% HgCl_2 is not reused by recycling. That is, approximately 800 ta^{-1} HgCl_2 is used for PVC production and 200 ta^{-1} of HgCl_2 waste is discharged into the environment, causing chronic poisoning that is severely harmful to human beings and the environment. Therefore, green mercury-free catalysts, which are mainly heterogeneous catalysts (e.g. HgCl_2 supported on activated carbon (AC),^[2] Au/C ,^[3–5] Cu-Bi/SiO_2 ,^[6] Au-Cu/C ,^[7]), are widely used. However, the preparation and post-processing of conventional metal-based catalysts for hydrohalogenation exhausts vast resources, which are toxic and involve high energy consumption.^[8] Therefore, searching promising materials for acetylene hydrochlorination that are environmentally acceptable and have low emissions is a topic of increased interest and importance for green chemical processes.


Metal-free heterogeneous catalysis using carbon combines environmental acceptability with inexhaustible resources, and is therefore an interesting alternative towards sustainable catalysis.^[8,9] The chemical properties of carbon nanotubes (CNTs) can be easily tailored by heteroatom functionalization at the edges, defects, or on strained regions, or by other methods. The incorporation of heteroatoms into CNTs (e.g., B, N, O, and P) tunes the electronic properties of the sp^2 carbons and affords significant improvements on their catalytic activities and electrochemical performances. For example, N-containing CNTs are effective alternatives to conventional metal-containing catalysts for oxidative dehydrogenation,^[8,10,11] insertion of oxygen atoms into acrolein,^[12] sulfur recovery from H_2S ,^[13] Friedel–Crafts reactions,^[14] biomass conversion,^[15] as well as the oxygen reduction reaction.^[16,17]

Suitable metal cations (e.g., Hg^{2+} , Au^{3+} , Bi^{3+} , Cu^{2+}) have been intensely investigated to obtain prominent reactivity towards C_2H_2 hydrochlorination.^[4,18] Generally, the electrophilic addition of HCl to acetylene is highly dependent on the electron affinity of the active site. If the electron affinity of carbon

[a] K. Zhou, Prof. Q. Zhang, Dr. J.-Q. Huang, G.-L. Tian, J.-C. Jia, Dr. M.-Q. Zhao, Prof. G.-H. Luo, Prof. F. Wei
Beijing Key Laboratory of Green Chemical Reaction Engineering and Technology
Department of Chemical Engineering
Tsinghua University, 100084 Beijing (PR China)
Fax: (+86) 10-6277-2051
E-mail: wf-dce@tsinghua.edu.cn

[b] Dr. B. Li, Prof. D. S. Su
Shenyang National Laboratory for Materials Science
Institute of Metal Research
Chinese Academy of Sciences
72 Wenhua Road, 110016 Shenyang (PR China)

[c] Prof. D. S. Su
Department of Inorganic Chemistry
Fritz Haber Institute of the Max Planck Society
Faradayweg 4–6, 14195 Berlin (Germany)
E-mail: dangsheng@fhi-berlin.mpg.de

 Supporting Information for this article is available on the WWW under <http://dx.doi.org/10.1002/cssc.201300793>.

can be as well tuned as the active metal cation by doping, then it is expected that the doped carbon may serve as a metal-free catalyst for hydrochlorination. Based on this consideration, we explored the idea of acetylene hydrochlorination on nitrogen-doped CNTs (NCNTs). The reasons why we selected CNTs as model catalysts are their unique physical/chemical properties,^[10,19] as well as the availability and low cost of bulk CNT samples with tunable electron affinity and stability below 400 °C in anaerobic atmosphere.^[10,20,21]

Our concept involved the use of NCNTs instead of traditional catalysts for C₂H₂ hydrochlorination, and an advanced understanding of the reactivity source and possible reaction mechanism. NCNTs were synthesized by chemical vapor deposition (CVD), and purified with HF and HCl aqueous solutions.^[21,22] The doping by nitrogen atoms altered the sp² carbon structure of the multiwalled CNTs (MWCNTs) and led to a cup-stacked structure (Figure 1a). A nitrogen content of 4.4% was determined by X-ray photoelectron spectroscopy (XPS) (Figure 1b). Five N–C bond species were fitted, corresponding to the pyridinic (398.3–399.8 eV), pyrrolic (400.1–400.5 eV), quaternary (401–402 eV), nitrogen oxide species (403.0–403.4 eV), and chemisorbed N (404.0–405.6 eV). The quaternary nitrogen is the biggest contributing nitrogen-containing form in NCNT1 (Figure 1b and Table 1).

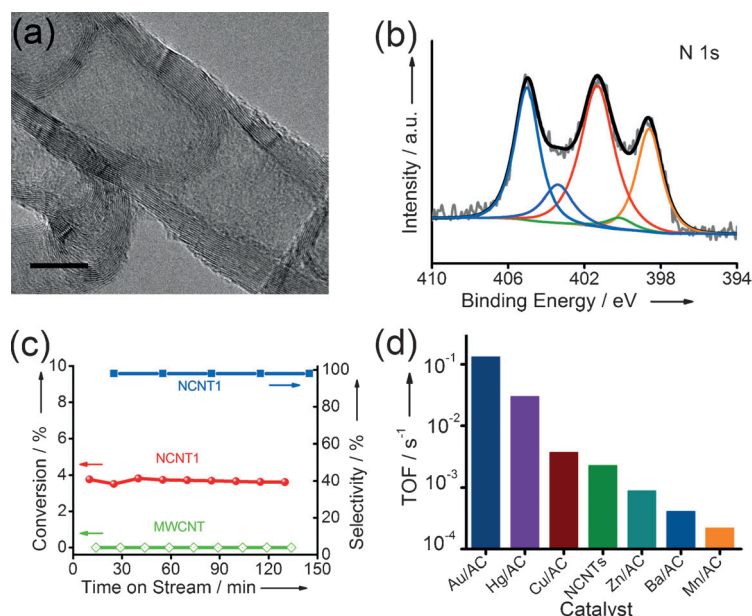
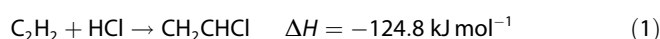


Figure 1. Hydrochlorination performance of the NCNT1 catalyst: (a) TEM image of NCNT1. The scale bar is 10 nm. (b) N 1s core-level spectrum of NCNT1. (c) The reactivity of C₂H₂ hydrochlorination on MWCNT and NCNT1 catalyst ($T = 180^{\circ}\text{C}$, GHSV- $(\text{C}_2\text{H}_2) = 180\text{ h}^{-1}$). (d) The TOFs of C₂H₂ hydrochlorination of Au, Hg, Cu, NCNT, Zn, Ba and Mn catalysts.

Sample	Conversion [%]	SSA [m ² g ⁻¹]	Nitrogen species [%]						
			pyridinic	pyrrolic	quaternary	N oxides	chemisorbed N	cyano-like	all
MWCNT	0	195	–	–	–	–	–	–	0
NCNT1	3.8	174	0.91	0.11	2.05	0.41	0.92	–	4.4
NCNT2	0	159	–	–	–	–	–	1.7	1.7
NCNT3	2.4	169	1.13	0.2	1.43	0.11	0.83	–	3.7
NCNT4	1.0	171	0.78	0.61	0.4	0.11	0.36	–	2.2
NCNT5	3.0	175	0.63	0.18	1.51	0.34	1.24	–	3.9
NCNT6	7.2	293	0.27	0.01	1.48	0.04	0.8	–	2.6

The activity towards hydrochlorination using MWCNT and NCNT1 was evaluated at 180 °C with 180 h⁻¹ of gas hourly space velocity (GHSV, C₂H₂ based) during 120 min. The hydrohalogenation reaction occurs as following:



The conversion of C₂H₂ was defined as the volume ratio of CH₂CHCl in the outer mixture of CH₂CHCl and C₂H₂. As shown in Figure 1c, NCNT1 had a remarkable better performance with an initial conversion of 3.8%, in contrast, no CH₂CHCl was detected when using MWCNTs. The selectivity towards CH₂CHCl was over 98% according to flame ionization detector (FID) and mass spectrometry (MS) detection. VCM was detected as the main product and only minor byproducts, around 0.5%, were formed according to the MS results (Figure S1). To compare the capacity of chlorinating C₂H₂ into VCM, the reactivity of metal-based catalysts (including Au, Hg, Cu, Zn, Ba, and Mn), as well as the NCNT catalyst is illustrated in Figure 1d. Compared to the metal catalysts, NCNTs have lower turnover frequency (TOF) than Au and Hg, but the value is significantly higher than that of Zn, Ba, and Mn, indicating the possibility to be a promising alternative route to produce vinyl chloride.

To gain new insights into the relationship between activity and N/O species, five other NCNT catalysts were used as control samples. NCNT2 was prepared by self-decomposition of azodiisobutyronitrile on MWCNTs to obtain only cyano-like groups, while NCNT3–6 with different nitrogen-containing functional groups were synthesized by CVD growth. Detailed synthesis procedures and related information can be found in Table 1 and in the Experimental section.

There is 3.5 wt% oxygen in MWCNTs, which can be ascribed to the contribution of hydroxyl and carboxylic groups, however, no hydrohalogenation reaction was observed when using the MWCNT catalyst. 1.4 wt% O and 1.7 wt% cyano-like N (Figure 2a) can be determined on NCNT2, but there was no C₂H₂ conversion. Therefore, the O species and cyano-like groups are not the origin of reactivity towards C₂H₂ hydrochlorination.

The NCNT1,3–6 obtained by CVD contained the above mentioned five N species (no cyano-like species). A typical XPS spectrum recorded from NCNT6 is

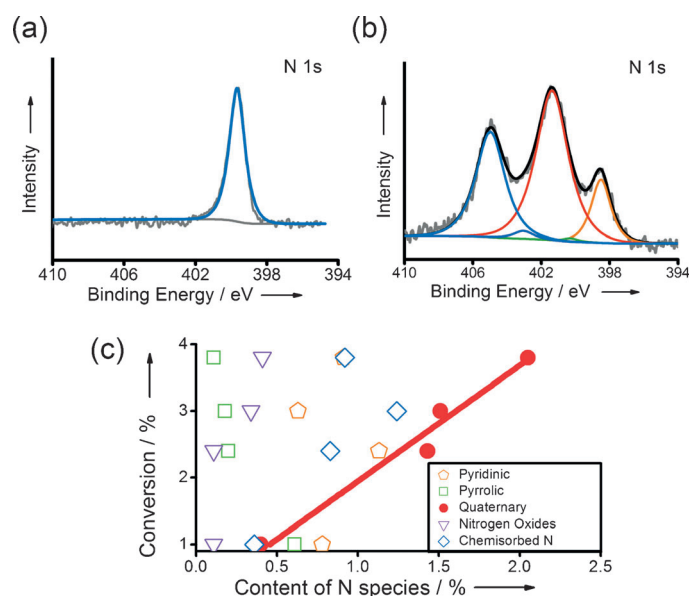


Figure 2. N 1s core-level spectrum of (a) NCNT2, and (b) NCNT6. (c) The fitting between nitrogen species content and reactivity towards hydrohalogenation.

shown in Figure 2b. NCNT1 and NCNT3–5 had a N content ranging from 1.7 to 4.4%, and a similar specified surface area. Figure 2c shows the relationship between N species and C₂H₂ conversion. The negative correlations between the content of pyridinic or pyrrolic N and the hydrohalogenation reactivity indicate that it is unlikely that these are important active sites. The surface-functionalized species of chemisorbed N are not the main reactivity source, similar to the cyano-based groups. Compared to NCNT1,3–5, NCNT6 has the smallest diameter of ca. 10 nm, the largest surface area of 293 m² g^{−1}, a quaternary N content of 1.48%, and a highest C₂H₂ conversion of 7.2% for hydrochlorination. For NCNTs with similar diameter and surface area (NCNT1,3–5), an increase of quaternary N content from 0.4% (NCNT4) to 1.43% (NCNT3) and further to 2.1% (NCNT1) corresponds to an increase of conversion of C₂H₂ from 1.0 to 2.4 to 3.8%, respectively (Figure 2c, Table 1). This is clearly a positive correlation between quaternary N content and activity. The TOF was calculated based on the quaternary nitrogen atoms. The TOF values of NCNT1 and NCNT6 are 1.5×10^{-3} and 2.3×10^{-3} s^{−1}, respectively.

The residual Fe catalysts in N-containing carbons were reported to play a role in some electrocatalytic reactions.^[17,23] Despite the negligible amounts of metal detected in the NCNTs used here (Table S1), the possible presence of trace Fe in the NCNTs might mislead the interpretation of the observed activity. Based on this consideration, we intentionally prepared a sample, NCNT7, with a Fe content of 1.4 wt% and tested it in C₂H₂ hydrohalogenation. The conversion data in Figure S2 did not show any significant improvement or deterioration, excluding the effect of Fe in the reaction.

In order to identify the pathway of hydrohalogenation on quaternary NCNTs, first-principles density functional theory (DFT) calculations were carried out (see Supporting Informa-

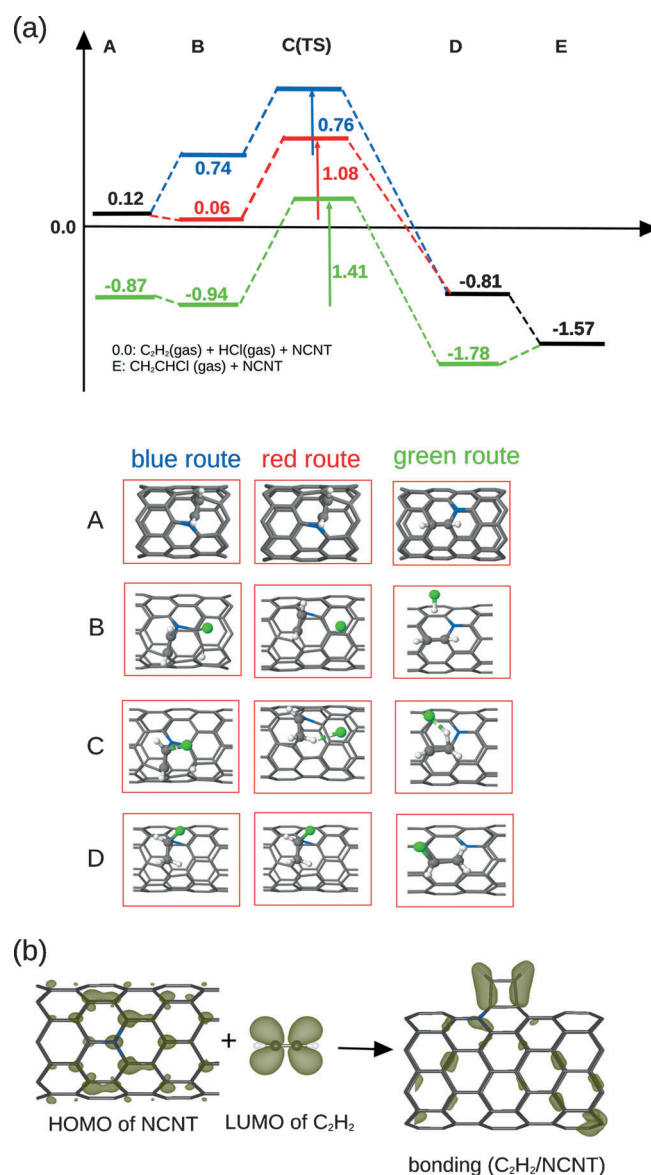


Figure 3. (a) The reaction pathways calculated from DFT calculations. TS: transition state. The zero point for energy represents the reactants (HCl and C₂H₂) in the gas phase and NCNT. The final step (E) is desorption of the product (CH₂CHCl) from NCNT. The structures A, B, C, D on three reaction pathways are also included. (b) The charge density of the HOMO orbital of NCNT, LUMO orbital of C₂H₂, and the bond formed between NCNT and C₂H₂. Carbon is gray, nitrogen is blue, and hydrogen is white. The isosurface value is 0.02 e Å³.

tion Figures S3–5 for details). The activation of alkynes by gold(III) has been well investigated in detail, including fully relativistic treatment, which provides a very significant reference value.^[24] Here, three different reaction pathways are shown in Figure 3a. All pathways start from the adsorption of C₂H₂ because the adsorption of HCl is very weak, as shown in Figure S5. The first step (A in Figure 3a) in reaction is most likely to be the addition of C₂H₂ to NCNT.^[25,26] There are two different structures of the adsorbed C₂H₂ molecule, which are distinguished from each other by the different binding sites. The C₂H₂ in the first structure binds at nitrogen and its nearest

carbon with an adsorption energy of 0.12 eV; the second structure has an adsorption energy of -0.87 eV and the adsorption sites are nitrogen's nearest and second-nearest carbons (more optimized structures in Figure S5). In the following, HCl approaches the NCNT, which represents step B in Figure 3a, and interacts with the adsorbed C_2H_2 to form the CH_2CHCl via two different ways: the first one is that the dissociative adsorbed HCl attacks the C_2H_2 , which is the blue pathway in Figure 3a; and the second one is that the HCl directly comes from the gas phase and binds weakly to NCNT, which is shown in the red and green pathways. The dissociative adsorption of HCl is endothermic by 0.74 eV in the blue pathway, and the HCl is weakly bound to the NCNT in the red and green pathways, with energies of -0.06 and -0.07 eV relative to step A, respectively. All reactants, C_2H_2 and HCl, on NCNT need to surmount an additional barrier to finally form CH_2CHCl . The barriers for the blue, red, and green pathways are 0.76, 1.08, and 1.41 eV respectively (the barrier represents the energy difference between transition state C and structure B). Inspecting the three transition state (TS) structures (bond distances in the TS structures are given in Table S2), the TS structures in the red and green pathways look similar. The H–Cl bond is breaking and the H atom of the HCl molecule tends to form a bond with C_2H_2 . For the TS structure in the blue pathway, instead of firstly forming a C–H bond, the Cl atom of HCl is heading to the adsorbed C_2H_2 and forms a C–Cl bond. After overcoming the barrier, a CH_2CHCl molecule is formed on NCNT as shown in step D and the adsorption energies are -0.81 eV for the blue and red pathways; -1.78 eV for the green pathway. The formed CH_2CHCl readily escapes from the NCNT, and the product is thus obtained. Comparing the three different pathways, the barrier in the blue pathway is the smallest one, however, the addition of HCl to NCNT is endothermic by 0.74 eV, which is thermodynamically much less favorable than the others. On the other hand, the difference between the red and green pathways lies in the different adsorbed structures of C_2H_2 which has an adsorption energy of 0.12 and -0.87 eV respectively. Due to this substantial difference in adsorption energies, the likely fate of adsorbed C_2H_2 on NCNT is the green pathway. Overall, the green pathway is the most favorable reaction route on NCNT for hydrochlorination of C_2H_2 , with a barrier of 1.41 eV. The barrier on $AuCl_3$ catalyst is calculated to be 0.92 eV from DFT calculations,^[25] which is smaller than the counterpart on NCNT by 0.49 eV. In view of this difference in the barrier energies, different performances are expected for Au and NCNT catalysts.

The reaction pathways from DFT calculations show that the first step of the reaction is adsorption of C_2H_2 , which to some extent determines which reaction pathway will proceed. The adsorption energies of C_2H_2 on undoped and nitrogen-doped CNTs were calculated, and the optimized adsorbed structures are shown in Figure S4. The optimized structures are very similar, but the adsorption energies show a noticeable difference. These are -0.36 and -0.87 eV for undoped and nitrogen-doped CNTs, respectively. Nitrogen doping enhances the adsorption of the C_2H_2 molecule compared to the undoped state. Furthermore, the stability of C_2H_2 on NCNT is attributed to for-

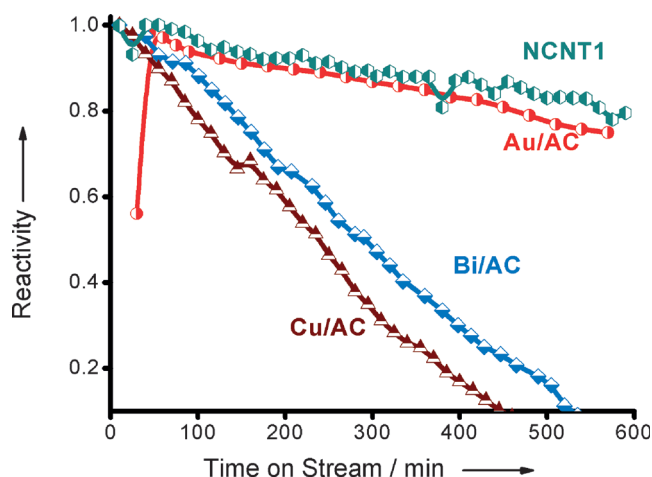


Figure 4. The stability of hydrochlorination on Au/AC, NCNT, Bi/AC, and Cu/AC catalysts ($GHSV(C_2H_2) = 180\text{ h}^{-1}$).

mation of covalent bonds between C_2H_2 and NCNTs as shown in Figure 3b, which is due to interactions between the highest occupied molecular orbital (HOMO) of NCNT and the lowest unoccupied molecular orbital (LUMO) of C_2H_2 . For $AuCl_3$ catalyst, the interaction is described between the HOMO of C_2H_2 and the LUMO of $AuCl_3$, which is opposite to situation with NCNTs. Because Au^{3+} is a strongly electrophilic, C_2H_2 behaves as an electron donor when interacting with $AuCl_3$. In fact, one of the reasons for the deactivation of $AuCl_3$ catalyst is the reduction of Au^{3+} to Au^0 , which is much more inert during the reaction.^[5,27] The doping by nitrogen increases the nucleophilicity of CNTs and enhances the interaction between the HOMO of NCNTs and the low-lying LUMO of C_2H_2 . Actually, it has been discussed that acetylene can interact with either electrophiles or nucleophiles depending on the corresponding reactants.^[28] From DFT calculations, different interaction mechanisms for C_2H_2 with NCNT and $AuCl_3$ catalysts are revealed.

The stability of NCNTs in the hydrohalogenation reaction, together with 0.1 wt% Au/AC, 5 wt% Bi/AC, and 2 wt% Cu/AC catalyst were evaluated. Figure 4 showed that Bi/AC and Cu/AC lost activity fast as the reaction proceeded, while the stability of NCNT1 was superior to the two non-precious-metal catalysts, and slightly better than that of the precious-metal catalyst Au/AC.

In summary, we demonstrated the hydrohalogenation reaction without use of a metal-containing catalyst: HCl is added to acetylene catalyzed by carbon nanotubes (CNTs). This finding could lead the way to a green, sustainable process for the PVC industry by replacing the contaminating $HgCl_2$ catalysts currently used in China. The activity is further improved by doping CNTs with nitrogen (NCNTs), increasing the nucleophilicity of the CNTs and thus enhancing interactions between the HOMO of NCNT and the low-lying LUMO of acetylene. The stability of the adsorbed C_2H_2 stems from covalent bonds formed between the HOMO of NCNTs and the LUMO of C_2H_2 . The acting mechanism differs from the mechanism when a metal-containing catalyst is used, and shows the potential of metal-free catalysis towards other reactions. In comparison to the

commonly used Hg-based catalysts, the metal-free NCNT catalyst offers promoted reactivity for sustainable hydrochlorination with a TOF value of $2.3 \times 10^{-3} \text{ s}^{-1}$.

Experimental Section

CNT synthesis: The MWCNTs were produced by fluidized-bed CVD on Fe-based catalyst.^[29] NCNT1 and NCNT3–5 were synthesized on a Fe/Mo/vermiculite catalyst and the reaction temperature was 750 °C under the protection of Ar and H₂.^[21] C₂H₄ and NH₃ were introduced as carbon source and nitrogen source, respectively, for NCNT growth. For NCNT1 synthesis, 10 g Fe/Mo/vermiculite catalyst was applied and the typical flow rates of Ar, H₂, C₂H₄, and NH₃ were 250, 200, 100, and 100 sccm, respectively. NCNT3–5 were synthesized with a similar procedure of NCNT1 except for the NH₃ flow rate, which was 45 %, 60 %, and 80 % of that in NCNT1 fabrication, respectively. NCNT6 was grown by using a CVD method with Fe–Mg–Al layered double hydroxide flakes as catalyst precursors and ethylene/acetonitrile as carbon/nitrogen feedstock,^[22] leading to double-helix CNTs. NCNT2 was obtained by treatment of MWCNTs with azobisisobutyronitrile (abbreviated as AIBN): a mixture of 0.4 g purified MWCNTs, 8.0 g AIBN, and 50 mL tetrahydrofuran was sonicated for 15 min and then transferred into a thermostatic water bath (50 °C) under stirring for 5 h. The mixture was then filtered by ethanol 3 times and dried for 24 h to obtain NCNT2.

MWCNT and NCNT1–5 all followed three purification cycles after the synthesis. Each cycle involved dispersion of CNTs in 6.0 mol L⁻¹ HCl aqua solution for 24 h, filtration by deionized water, dispersion in 6.0 mol L⁻¹ HF aqua solution, and filtration by deionized water. The purified CNTs were dried at 120 °C over 12 h before further use. NCNT7 and NCNT5 came from the same raw N-CNTs, while NCNT7 was purified by HF aqua solution to remove only the substrates, therefore, 1.4 wt % Fe was still preserved in the as-obtained sample.

Catalytic performance evaluation: The 0.3 g CNT catalyst samples were evaluated as follows: loaded into the quartz tube, dried under 10 sccm N₂ atmosphere at 120 °C for 10 min, activated under 10 sccm HCl atmosphere at 180 °C for 15 min, and reacted under the flow of C₂H₂ and HCl at 180 °C for 180 min ($Q_{\text{acetylene}}/Q_{\text{HCl}} = 1:1.1$). The GHSV was 180 h⁻¹ calculated by the value of $Q_{\text{acetylene}} (\text{mL min}^{-1})/V_{\text{CNTs}} (\text{mL})$, depending on the volume of the samples.

Acknowledgements

We appreciate great help from Mr. Wen-Hu Hu and Jiang-Kun Si. This work was supported by National Basic Research Program of China (2011CB932602) and Key Technologies R&D Program of China (2008BAB41B02, 2012AA062901). B.L. is supported by SYN-L-T.S. K Research Fellowship. B.L. thanks financial grant from the China Postdoctoral Science Foundation (2012M511186) and computing time from ShenYang Branch, Supercomputing Center of CAS. B.L. and D.S.S. acknowledge the financial support from MOST (2011CBA00504), NSFC of China (21133010, 51221264, 21261160487).

Keywords: carbon nanotubes • ethene • hydrochlorination • mercury • sustainable chemistry

- [1] J. Bing, C. Li, *Polyvinyl Chloride* **2011**, 39, 1–8.
- [2] R. E. Lynn, K. A. Kobe, *Ind. Eng. Chem.* **1954**, 46, 633–643; X. B. Wei, H. B. Shi, W. Z. Qian, G. H. Luo, Y. Jin, F. Wei, *Ind. Eng. Chem. Res.* **2009**, 48, 128–133.
- [3] G. J. Hutchings, R. Joffe, *Appl. Catal.* **1986**, 20, 215–218; G. J. Hutchings, *Catal. Today* **2002**, 72, 11–17; M. Conte, C. J. Davies, D. J. Morgan, T. E. Davies, A. F. Carley, P. Johnston, G. J. Hutchings, *Catal. Sci. Technol.* **2013**, 3, 128–134; G. J. Hutchings, *Top. Catal.* **2008**, 48, 55–59; M. Conte, C. J. Davies, D. J. Morgan, T. E. Davies, D. J. Elias, A. F. Carley, P. Johnston, G. J. Hutchings, *J. Catal.* **2013**, 297, 128–136; A. S. K. Hashmi, M. Buehrle, *Aldrichimica Acta* **2010**, 43, 27–33; M. Zhu, L. Kang, Y. Su, S. Zhang, B. Dai, *Can. J. Chem.* **2013**, 91, 120–125; H. Zhang, B. Dai, X. Wang, W. Li, Y. Han, J. Gu, J. Zhang, *Green Chem.* **2013**, 15, 829–836; B. Nkosi, N. J. Coville, G. J. Hutchings, *J. Chem. Soc. Chem. Commun.* **1988**, 71–72; B. Nkosi, N. J. Coville, G. J. Hutchings, *Appl. Catal.* **1988**, 43, 33–39.
- [4] G. J. Hutchings, *J. Catal.* **1985**, 96, 292–295.
- [5] B. Nkosi, N. J. Coville, G. J. Hutchings, M. D. Adams, J. Friedl, F. E. Wagner, *J. Catal.* **1991**, 128, 366–377.
- [6] K. Zhou, J. C. Jia, X. G. Li, X. D. Pang, C. H. Li, J. Zhou, G. H. Luo, F. Wei, *Fuel Process. Technol.* **2013**, 108, 12–18.
- [7] S. J. Wang, B. X. Shen, Q. L. Song, *Catal. Lett.* **2010**, 134, 102–109.
- [8] D. S. Su, J. Zhang, B. Frank, A. Thomas, X. Wang, J. Paraknowitsch, R. Schloegl, *ChemSusChem* **2010**, 3, 169–180.
- [9] D. R. Dreyer, C. W. Bielawski, *Chem. Sci.* **2011**, 2, 1233–1240; J. H. Bitter, *J. Mater. Chem.* **2010**, 20, 7312–7321; D. S. Yu, E. Nagelli, F. Du, L. M. Dai, *J. Phys. Chem. Lett.* **2010**, 1, 2165–2173.
- [10] B. Frank, J. Zhang, R. Blume, R. Schloegl, D. S. Su, *Angew. Chem.* **2009**, 121, 7046–7051; *Angew. Chem. Int. Ed.* **2009**, 48, 6913–6917.
- [11] A. Rinaldi, J. Zhang, B. Frank, D. S. Su, S. B. A. Hamid, R. Schlögl, *ChemSusChem* **2010**, 3, 254–260; X. Liu, B. Frank, W. Zhang, T. P. Cotter, R. Schlögl, D. S. Su, *Angew. Chem.* **2011**, 123, 3376–3380; *Angew. Chem. Int. Ed.* **2011**, 50, 3318–3322; J. Zhang, R. Wang, E. Z. Liu, X. F. Gao, Z. H. Sun, F. S. Xiao, F. Girgsdies, D. S. Su, *Angew. Chem.* **2012**, 124, 7699–7704; *Angew. Chem. Int. Ed.* **2012**, 51, 7581–7585.
- [12] B. Frank, R. Blume, A. Rinaldi, A. Trunschke, R. Schlögl, *Angew. Chem.* **2011**, 123, 10408–10413; *Angew. Chem. Int. Ed.* **2011**, 50, 10226–10230.
- [13] K. Chizari, A. Deneuve, O. Ersen, I. Florea, Y. Liu, D. Edouard, I. Janowska, D. Begin, P.-H. Cuong, *ChemSusChem* **2012**, 5, 102–108.
- [14] F. Goettmann, A. Fischer, M. Antonietti, A. Thomas, *Angew. Chem.* **2006**, 118, 4579–4583; *Angew. Chem. Int. Ed.* **2006**, 45, 4467–4471.
- [15] J. P. Tessonnier, A. Villa, O. Majoulet, D. S. Su, R. Schlögl, *Angew. Chem.* **2009**, 121, 6665–6668; *Angew. Chem. Int. Ed.* **2009**, 48, 6543–6546.
- [16] S. B. Yang, L. J. Zhi, K. Tang, X. L. Feng, J. Maier, K. Mullen, *Adv. Funct. Mater.* **2012**, 22, 3634–3640; D. S. Yu, Q. Zhang, L. M. Dai, *J. Am. Chem. Soc.* **2010**, 132, 15127–15129.
- [17] Y. G. Li, W. Zhou, H. L. Wang, L. M. Xie, Y. Y. Liang, F. Wei, J. C. Idrobo, S. J. Pennycook, H. J. Dai, *Nat. Nanotechnol.* **2012**, 7, 394–400.
- [18] C. Marco, H. Graham, *Modern Gold Catalyzed Synthesis*, Wiley-VCH, **2012**.
- [19] J. Zhang, D. Su, A. Zhang, D. Wang, R. Schlögl, C. Hebert, *Angew. Chem.* **2007**, 119, 7460–7464; *Angew. Chem. Int. Ed.* **2007**, 46, 7319–7323; J. Zhang, X. Liu, R. Blume, A. Zhang, R. Schlögl, D. S. Su, *Science* **2008**, 322, 73–77.
- [20] J. A. Maciá-Agulló, D. Cazorla-Amoros, A. Linares-Solano, U. Wild, D. S. Su, R. Schlögl, *Catal. Today* **2005**, 102, 248–253.
- [21] J. Q. Huang, M. Q. Zhao, Q. Zhang, J. Q. Nie, L. D. Yao, D. S. Su, F. Wei, *Catal. Today* **2012**, 186, 83–92.
- [22] G. L. Tian, M. Q. Zhao, Q. Zhang, J. Q. Huang, F. Wei, *Carbon* **2012**, 50, 5323–5330.
- [23] D. S. Su, G. Q. Sun, *Angew. Chem.* **2011**, 123, 11774–11777; *Angew. Chem. Int. Ed.* **2011**, 50, 11570–11572.
- [24] C. M. Krauter, A. S. K. Hashmi, M. Pernpointner, *ChemCatChem* **2010**, 2, 1226–1230; M. Lein, M. Rudolph, S. K. Hashmi, P. Schwerdtfeger, *Organometallics* **2010**, 29, 2206–2210; M. Pernpointner, A. S. K. Hashmi, *J. Chem. Theory Comput.* **2009**, 5, 2717–2725.
- [25] J. L. Zhang, Z. H. He, W. Li, Y. Han, *RSC Adv.* **2012**, 2, 4814–4821.
- [26] M. Conte, A. F. Carley, C. Heirene, D. J. Willock, P. Johnston, A. A. Herzog, C. J. Kiely, G. J. Hutchings, *J. Catal.* **2007**, 250, 231–239.
- [27] A. S. K. Hashmi, L. Schwarz, J. H. Choi, T. M. Frost, *Angew. Chem.* **2000**, 112, 2382–2385; *Angew. Chem. Int. Ed.* **2000**, 39, 2285–2288; A. S. K.

- Hashmi, T. M. Frost, J. W. Bats, *J. Am. Chem. Soc.* **2000**, *122*, 11553–11554; A. S. K. Hashmi, M. C. Blanco, D. Fischer, J. W. Bats, *Eur. J. Org. Chem.* **2006**, 1387–1389.
- [28] A. S. Hashmi, *Gold Bull.* **2003**, *36*, 3–9.
- [29] Q. Zhang, J. Q. Huang, W. Z. Qian, Y. Y. Zhang, F. Wei, *Small* **2013**, *9*, 1237–1265; Q. Zhang, J. Q. Huang, M. Q. Zhao, W. Z. Qian, F. Wei, *ChemSusChem* **2011**, *4*, 864–889.

Received: August 2, 2013

Revised: November 13, 2013

Published online on January 23, 2014
